Article

Exercise alters transcriptional profiles of senescence and gut barrier integrity in intestinal crypts of aging mice

Check for updates

Hyeonuk Jeon[1,2,3,11], Siyeon Lee[4,11], Yumin Kim[5], Yeongmin Kim[5], Soyeon Shin[5], Yoseob Lee[6], Minki Kim[7], Eunbin Ko[8], Eunsu Lee[9], Brian Min Song[10], Hojeong Choi[1,2,3], Nahee Hwang[6], Se-eun Han[2,6], Byungjin Hwang[2,6], Jae-Woo Kim[1,3], Chang-Myung Oh[5] ✉ & Sungsoon Fang[2,3,6] ✉

Senescence is the gradual process of aging in tissues and cells, and a primary cause of aging-associated diseases. Among them, intestinal stem cells (ISCs) experience exhaustion during aging, leading to reduced regenerative capacity in the intestinal crypt, which impairs intestinal function and contributes to systemic health issues. Given the critical role ISCs play in maintaining intestinal homeostasis, preventing their senescence is essential for preserving intestinal function. Among the various strategies proposed to slow cellular senescence, regular exercise has emerged as one of the most well-known and widely accepted interventions. Here, we examined how exercise affects the small intestine in an aging mouse model. Using single-cell RNA sequencing, we found that signaling pathways and gene expression related to DNA replication and cell cycle progression were upregulated in ISCs. Additionally, genes promoting ribosome biogenesis showed increased expression in both ISCs and transit amplifying cells. Exercise also recovered Wnt signaling inhibition, potentially influencing ISC differentiation. Furthermore, exercise increased Reg3g expression in Paneth cells and improved gut barrier function, contrasting with findings from a diet-induced obese mouse model. This suggests that regular exercise helps inhibit the aging of ISCs in multiple ways, contributing to the maintenance of intestinal homeostasis.

Senescence is a complex biological process that characterized by the gradual decline in cellular and tissue function, leading to increased susceptibility to disease and a decrease in overall vitality. Among the interventions studied to combat senescence, exercise is widely recognized for its myriad health benefits, including its potential to delay the aging process. Regular physical activity has been shown to improve cardiovascular health, enhance metabolic function, and extend lifespan[1–3]. There are numerous factors that can accelerate senescence, but when considering exercise, one of the most straightforward connections is with metabolic dysfunction. Existing research has shown that metabolic dysfunction, such as hyperglycemia and insulin resistance caused by senescence or excessive consumption of a western diet, can accelerate senescence by inducing oxidative stress and impaired signaling[4–7].

Among various tissue, the intestine plays a crucial role in nutrient absorption, immune function, and overall health[8,9]. It is also a site where functional alterations frequently occur due to metabolic diseases or aging. In obese individuals, it is well-documented that the intestinal barrier function decreases, leading to a phenomenon known as 'gut leakage'[10,11]. At the cellular level within the intestinal epithelium, the proliferation and differentiation of intestinal stem cells (ISCs) are impaired, and the secretion of antimicrobial peptides like Reg3g decreases[12–14]. As aging progresses, ISCs become exhausted, and the transit time of food through the intestine

[1]Department of Biochemistry and Molecular Biology, Yonsei University College of Medicine, Seoul, Republic of Korea. [2]Graduate School of Medical Science, Brain Korea 21 Project, Yonsei University College of Medicine, Seoul, Republic of Korea. [3]Chronic Intractable Disease for Systems Medicine Research Center, Yonsei University College of Medicine, Seoul, Republic of Korea. [4]Department of Life Science and Biotechnology, Underwood Division, Underwood International College, Yonsei University, Seoul, Republic of Korea. [5]Department of Biomedical Science and Engineering, Gwangju Institute of Science and Technology, Gwangju, Republic of Korea. [6]Department of Biomedical Sciences, Yonsei University College of Medicine, Seoul, Republic of Korea. [7]Harold C. Simmons Comprehensive Cancer Center, University of Texas Southwestern Medical center, Dallas, TX, USA. [8]Faculty of Life Sciences and Medicine, King's College London, London, United Kingdom. [9]Department of Medicine, Yonsei University College of Medicine, Seoul, Republic of Korea. [10]Hallym University College of Medicine, ChunCheon, Gangwon-do, Republic of Korea. [11]These authors contributed equally: Hyeonuk Jeon, Siyeon Lee. ✉e-mail: cmoh@gist.ac.kr; sfang@yuhs.ac

1

increases, which leads to a decline in intestinal function[15,16]. This suggests a strong correlation between metabolic syndrome and aging, underscoring the need to investigate whether regular exercise can improve common aspects of both conditions. While exercise is well-known for its ability to delay aging across various organ, the specific changes that occur in the intestine due to exercise remain poorly understood[1,17–19].

The intestinal crypt, located between villi and forming part of the crypt-villus unit, is the fundamental unit of the intestinal epithelium[20]. The intestinal crypt contains various cells, including ISCs, Paneth cells (PCs), Goblet cells (GCs), enteroendocrine cells (EECs), and tuft cells, all of which regulate epithelial homeostasis and contribute to interactions with the microbiome and immune responses[21,22]. Due to this, we aimed to investigate how exercise influences the homeostasis of the intestinal crypt to understand its impact on maintaining gut health in the small intestine. Additionally, we compared the intestinal crypts of obese mice to determine which aspects were improved through exercise.

Aging also affects ISCs by reducing their proliferative and regenerative capacities, which are essential for maintaining tissue homeostasis. Studies have shown that aged ISCs exhibit reduced potential for self-renewal and differentiation, a hallmark of cellular senescence[23]. Senescence in ISCs is influenced by factors such as DNA damage, with radiation-induced DNA damage triggering the DNA damage response. This process can lead to cell cycle arrest or apoptosis, depending on the severity of the damage. A key player in cell cycle arrest is p21, a cyclin-dependent kinase inhibitor that blocks CDK2 activity, halting cell cycle progression and promoting senescence through p53-dependent and independent mechanisms[24,25]. Overexpression of p21 further drives the senescence phenotype by upregulating senescence markers and downregulating proliferative genes.

In addition to DNA damage-induced senescence, chronic inflammation plays a crucial role in driving ISCs dysfunction, particularly in obesity-associated metabolic stress. Pro-inflammatory cytokines such as TNF-α, IL-6, and IL-1β are key mediators of inflammation-induced senescence, activating pathways such as NF-κB and JAK-STAT, which lead to sustained p21 and p16INK4a expression, promoting cell cycle arrest and stem cell exhaustion[26,27]. This chronic inflammatory state, often observed in obesity, is exacerbated by senescence-associated secretory phenotype (SASP), where senescent cells secrete cytokines, chemokines, and matrix metalloproteinases that further propagate inflammation and impair intestinal barrier integrity. Notably, obesity-induced gut inflammation has been linked to increased gut permeability, allowing microbial-derived endotoxins such as lipopolysaccharides (LPS) to enter circulation and amplify systemic inflammation[28]. This feedback loop accelerates ISC dysfunction, leading to impaired epithelial regeneration and gut barrier deterioration, hallmarks of both obesity-related intestinal dysfunction and aging-associated decline. Given the role of inflammation in perpetuating senescence, interventions such as exercise may mitigate these effects by reducing pro-inflammatory cytokine signaling, restoring ISC function, and enhancing gut barrier integrity[29].

Cell cycle arrest is defining feature of cellular senescence and is regulated by tumor suppressor pathways such as the p53/p21 and p16INK4a/Rb axes[30]. These pathways ensure that damaged or stressed cells do not proliferative, preventing the spread of mutations. However, the accumulation of senescent cells over time can disrupt this process, contributing to age-related pathologies[31]. Understanding how aging impacts the cell cycle and senescence in ISCs is essential for devising strategies to maintain intestinal function during aging.

The differentiation of ISCs is regulated by the Notch and Wnt signaling pathways, which direct differentiation into specific cell types[32–34]. ISCs influenced by the Notch signaling pathways are directed to differentiate into cell types with absorptive characteristics, such as enterocytes[32,35]. Conversely, when influenced by the Wnt signaling pathway, ISCs are directed to differentiate into secretory cell types, including Paneth cells, goblet cells, and enteroendocrine cells[33,36]. Furthermore, as aging progresses, Wnt signaling in ISCs decreases, and it has been reported that canonical Wnt signaling alleviates aging in ISCs[23]. This suggests that among the various changes

exercise induces in the gut, the involvement of Wnt signaling should also be examined.

Understanding how exercise influences intestinal health at the cellular level could provide valuable insights into strategies for promoting healthy aging and preventing age-associated intestinal disorders. In this study, we aim to elucidate the effects of exercise on cellular senescence within the intestinal crypts of aged mice. By utilizing single-cell RNA sequencing, we compare the transcriptome profiles of intestinal crypt from sedentary aged mice to those subjected to regular exercise. And then, we examined whether the so-called "Hallmarks of aging", such as cell cycle arrest, stem cell exhaustion, and the expression of senescence markers, were improved[15,37]. We also examined whether the increased intestinal permeability observed in the intestinal epithelium of obese mice was improved through exercise, as well as whether the secretion of antimicrobial peptides and other secretory molecules was enhanced.

Results
Exercise enhances physical performance and reduces the expression of senescence marker genes in the intestine
To investigate the changes occurring in the intestines of aged mice subjected to regular exercise, we divided the mice (22 months-old) into control ($n = 6$) and exercise group ($n = 6$) and conducted an 8-weeks experiments. During this period, we performed power tests and endurance tests twice. At the end of the experiment, the mice were sacrificed, and intestinal crypts were isolated from the ileum for single-cell RNA sequencing. (Fig. 1a). When comparing body weight changes between the two groups, both groups showed a gradual decrease in weight over time (Supplementary Fig. 1a). At the end of the experiment, the exercise group exhibited a more significant reduction in body weight compared to the control group (Supplementary Fig. 1b). However, this change was considered a natural outcome of the increased physical activity. Notably, it was observed that the exercise group showed improved physical performance. The power test, which measures short-term exercise capacity, and the endurance test, which measures stamina, both indicated that these factors increased in the exercise group compared to the control group, with greater improvements seen as the duration of exercise increased (Fig. 1b, c).

To assess changes in mRNA levels, we performed single-cell RNA sequencing on 3867 cells, with each group consisting of 3 biological replicates (Fig. 1d). On average, each cell expressed 5000 genes (Fig. 1e). The vehicle group consisted of 1834 cells, and the exercise group of 2033 cells, indicating a minimal difference in cell numbers between the two groups. Considering transit amplifying (TA) cells as a distinct cell type, we identified a total of six cell types using their respective marker genes (Fig. 1f). Among the cell types constituting the intestinal crypt, tuft cells were not detected. First, we investigated whether exercise could delay the progression of aging in the intestine by assessing the enrichment of the SenMayo, which comprises genes highly expressed in senescent cells[38]. Although the entire intestinal crypt did not show a significant change in SenMayo enrichment depending on exercise, a reduction was observed in ISCs and TA cells (p value < 0.01, Normalized enrichment score < −1.67) (Fig. 1g). Specifically, 10 genes (*Bmp2, Egf, Ccl5, Ccl4, Fgf1, Ccl20, Gem, Nrg1, Tnfrsf11b, Vegfa*) within the SenMayo showed a marked decrease in expression in ISCs (Fig. 1h). These findings indicate that exercise reduces the expression of genes commonly upregulated in senescent cells.

Exercise restores cell cycle progression in ISCs
Based on the previous finding, we used the PROGENy package to gain an overview of the changes in signaling within ISCs in the exercise group[39]. The heatmap revealed an increase in signaling pathways related to proliferation, such as EGFR, VEGF, and Estrogen. Additionally, there was a noticeable decrease in inflammation-related pathways like JAK-STAT, TNF, NF-κB (Fig. 2a). These results suggest that exercise may be associated with promoting stem cell cycle progression. The comparison of gene expressions using violin plots further supported this hypothesis. The expression of two genes involved in the transition from the G1 to the S phase of the cell cycle
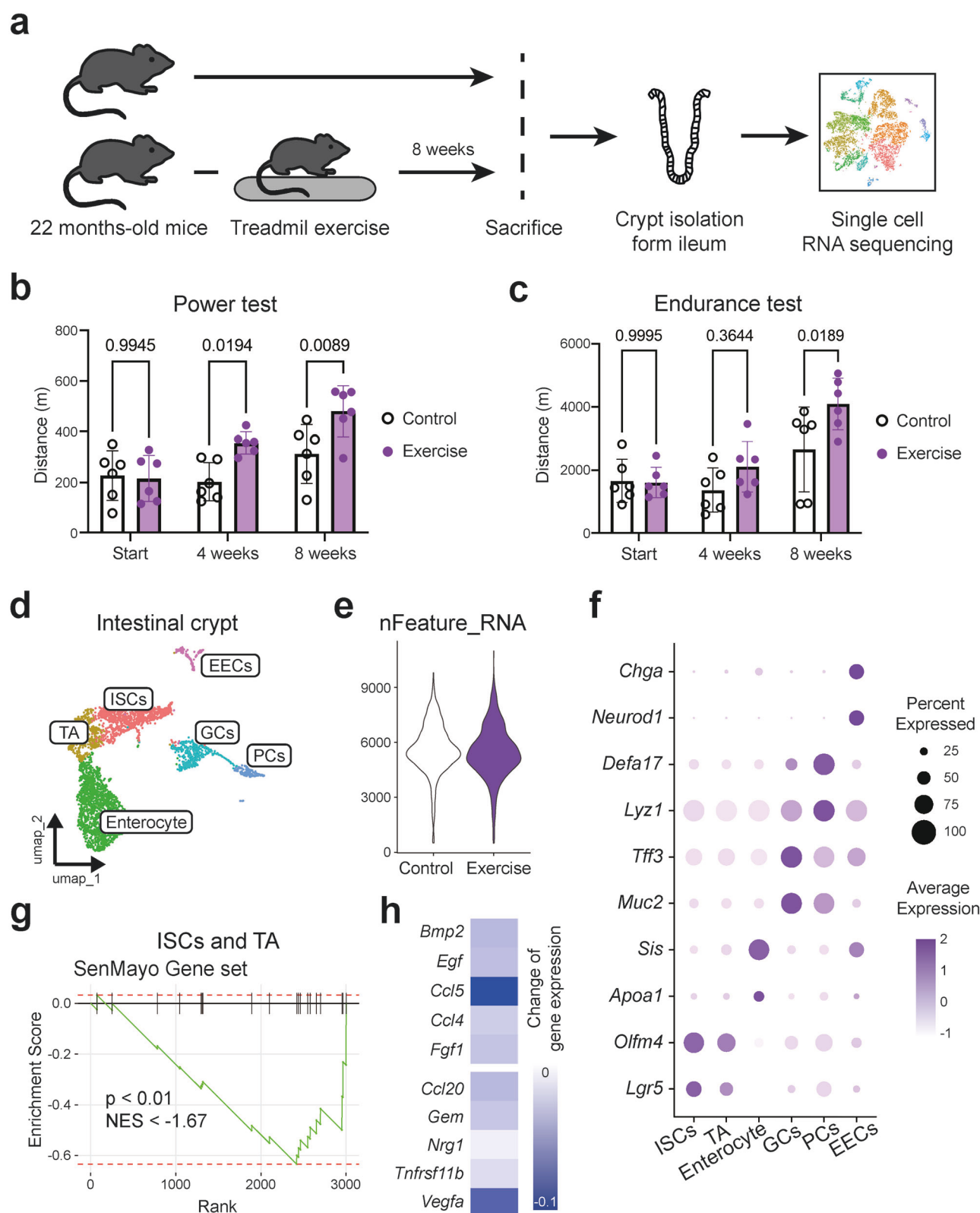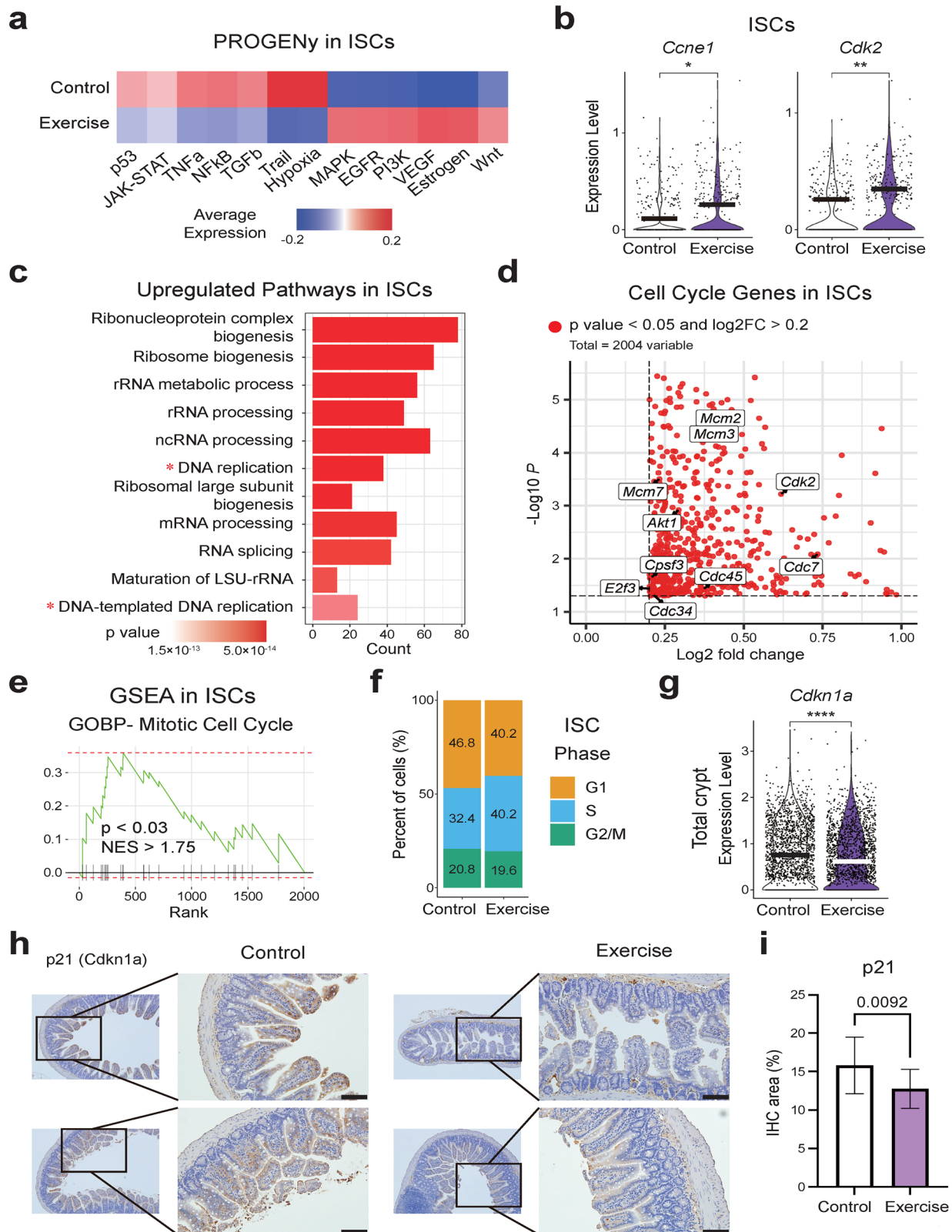
Fig. 1 | Exercise induces a reduction in senescence marker expression in the small intestine. a Experimental design illustrating the study setup. **b**, **c** Results of power test and endurance test. Data are shown as mean ± S.D. **d** UMAP plot showing the clustering of various cell types identified in the intestinal crypt. **e** Displaying the distribution of nFeature_RNA in crypt cells. **f** Dot plot indicating the expression levels and percentage of expression of key marker genes across the identified cell types. **g** Enrichment of ISCs and TA cells of SenMayo gene set. **h** Differential expression of selected SenMayo gene set in ISCs and TA cells between the control and exercise group. *P* value was calculated by 2-way ANOVA. Percent Expressed = Ratio of cells expressing the gene of interest among the total cells. *P* = p value, NES = Normalized enrichment score.

a PROGENy in ISCs

b ISCs — *Ccne1*, *Cdk2*

c Upregulated Pathways in ISCs

d Cell Cycle Genes in ISCs

p value < 0.05 and log2FC > 0.2
Total = 2004 variable

e GSEA in ISCs — GOBP- Mitotic Cell Cycle
p < 0.03
NES > 1.75

f ISC Phase — G1, S, G2/M

g *Cdkn1a*

h p21 (Cdkn1a) — Control / Exercise

i p21 — 0.0092

(*Ccne1*, *Cdk2*) was found to be increased (Fig. 2b). A pathway analysis was also conducted to investigate the changes occurring in ISCs during exercise. The analysis revealed an upregulation of signaling pathways related to DNA replication (Fig. 2c). Furthermore, when differentially expressed gene were extracted from ISCs, an increase in the expression of genes associated with cell cycle progression was observed (Fig. 2d). Using MsigDB to verify the enrichment of individual pathways, we observed an increase in the mitotic cell cycle (p value < 0.03, Normalized enrichment score > 1.75) in the exercise group (Fig. 2e). These results also influenced the cell cycle phase distribution of ISCs; while the proportion of cells in the G2/M phase showed little change between groups, the proportion of cells in the G1 phase decreased, and the proportion of cells in the S phase increased (Fig. 2f).

Fig. 2 | Enhanced proliferation pathways in small intestinal crypt cells of exercised mouse. a The PROGENy analysis of signaling pathways in ISCs from control and exercised mice. **b** The expression levels of *Ccne1* and *Cdk2*. The log(fold change) (log(FC)) values of the listed genes are greater than or equal to 0.2. **c** Upregulated pathways in ISCs from exercised mice, highlighting the increased activity in pathways related to DNA replication. **d** Volcano plot displaying the differentially expressed genes associated with cell cycle progression in ISCs. **e** GSEA of ISCs showing a significant enrichment of pathways related to mitotic cell cycle in the exercise group. **f** Representing the distribution of cell cycle phases in ISCs from control and exercised mice. **g** Expression level of *Cdkn1a* (p21). **h** IHC results from the small intestine. The smaller image on the left was taken at 10× magnification, with a portion re-captured at 20× magnification. The area is marked with a black square. The black bar represents the scale bar, indicating 100 μm. **i** IHC area (The ratio between the total tissue area and the area where the protein was detected) between two groups. Data are shown as mean ± S.D. *P* value was calculated using Nested t-test. *$P < 0.05$, **$P < 0.01$, ****$P < 0.0001$. P = p value, NES = Normalized enrichment score. The black and white bar in the middle of the violin plot represents the mean expression level for each group.

Given the observed decrease in cell cycle arrest markers and increased cell cycle progression, we further analyzed the expression of the well-known senescence markers p16 (Cdkn2a) and p21 (Cdkn1a), both of which are key regulators of cell cycle arrest[40]. First, we found a decrease in expression p21 in exercise group; however, p16 expression was not readily detected across the intestine in our data (Fig. 2g, Supplementary Fig. 2a). To validate these findings, we conducted immunohistochemistry (IHC) on ileum. Consistent with the RNA-seq data, we observed a marked reduction in p21 expression in the exercise group (Fig. 2h, I, Supplementary Data 1). In contrast, p16 expression showed no notable changes in ileum (Supplementary Fig. 2b, Supplementary Data 2). Additionally, we examined the expression of γ-H2AX, a DNA damage marker associated with aging[41]. However, we did not observe a significant difference between the two groups (Supplementary Fig. 2c, Supplementary Data 3). This further supports the notion that exercise mitigates cellular senescence in ISCs by promoting cell cycle progression and reducing senescence associated with cell cycle arrest.

Exercise promotes ribosome biogenesis in ISCs and TA cells

Cell cycle arrest due to senescence can occur for various reasons, one of which is impaired ribosome biogenesis caused by intrinsic cellular factors[42,43]. In senescent cells, the expression of genes involved in ribosome biogenesis, such as RSL1D1 and EBP2, is reduced, leading to this outcome[42,44]. This reduction inhibits the activity of cyclin and cyclin-dependent kinases, particularly cyclin D1 (*Ccnd1*) and CDK4, thereby inducing cellular senescence[42,45–47]. Also, the activation of p53 can induce replicative stress in cells, leading to the onset of senescence[48]. Consequently, given the observed increased in signaling pathways and factors related to cell cycle progression in the ISCs of the exercise group, we hypothesized that ribosome biogenesis might also be affected in some manner.

Transit-amplifying (TA) cells play a crucial role in maintaining intestinal homeostasis by acting as a rapidly proliferating intermediary between ISCs and differentiated epithelial cells. Located above the ISC niche in the intestinal crypts, TA cells undergo several rounds of division before committing to either an absorptive (enterocytes) or secretory (Paneth, goblet, enteroendocrine) lineage[49]. Their proliferation rate is tightly regulated by key signaling pathways such as Wnt, Notch, and EGFR, which coordinate the balance between cell renewal and differentiation[50]. Given their role as the main proliferative and differentiative force in the intestinal epithelium, understanding how exercise impacts TA cell dynamics is essential for uncovering its effects on intestinal regeneration, differentiation, and senescence.

Pathway analysis of ISCs and TA cells revealed that signaling pathways associated with ribosome biogenesis were increased in the exercise group (Fig. 3a, b). Additionally, signaling pathways related to rRNA were also elevated (Fig. 3a, b). This suggests that the increased expression of various genes involved in ribosome biogenesis contributed to these findings (Fig. 3c). Furthermore, we observed that the expression of key factors in ribosome biogenesis, *Rsl1d1* and EBP2 (*Ebna1bp2*), was also elevated in the exercise group (Fig. 3c, d). Also, we examined the changes in the expression of p53, CDK4, and CCND1, which are known to influence ribosomal protein formation[42]. Specifically, the expression of p53 (*Trp53*) decreased in the exercise group, although the expression of *Mdm2*, which binds to p53 and induces cell cycle arrest and senescence, remained unchanged[51,52] (Fig. 3e). Additionally, the expression of *Cdk4*

and *Ccnd1* was increased (Fig. 3f). These findings indicated that the promotion of ribosome biogenesis plays a crucial role in alleviating cell cycle arrest in ISCs in exercise group, and this effect also contributes to the improvement in the expression of various senescence-related genes.

Exercise reduces the expression of Wnt signaling inhibitors, impacting intestinal homeostasis

As previously mentioned, the differentiation of ISCs is influenced by Notch and Wnt signaling pathways[32,36]. Given this, we investigated whether exercise also affects the direction of ISC differentiation in aging mouse model. In ISCs and TA cells, an analysis of the genes involved in Notch signaling (*Notch1-3*, *Hes1*, *Olfm4*, *Adam10*) revealed that there was a general trend of decreases; However, these changes were not significant except for *Notch2* (Fig. 4a). Similarly, when examining the changes in genes involved in Wnt signaling (*Wnt3*, *Ctnnb1*, *Tcf4*, *Tcf7l2*), the expression of *Wnt3* and β-catenin (*Ctnnb1*) showed an increasing trend, but these changes were not significant (Fig. 4b). However, we observed that the expression of factors inhibiting Wnt signaling was decreased. Specifically, the expression of *Apc*, which is known to inhibit Wnt signaling by promoting the degradation of β-catenin, was reduced[53,54] (Fig. 4b). Additionally, the expression of *Rnf43* and *Znrf3*, which induce the degradation of Wnt receptors through ubiquitination, was also decreased[55,56] (Fig. 4b, c). Thus, while it is difficult to conclude that exercise directly induces an increase in the expression of molecules involved in Wnt signaling in ISCs, it can be inferred that exercise reduces the expression of Wnt signaling inhibitors, thereby maintaining or indirectly promoting Wnt signaling activity.

To determine whether these changes influence the differentiation trajectory of ISCs, we first examined the number and proportion of cell types constituting the intestinal crypt. In the exercise group, both the number and proportion of enterocytes were smaller than the control group, while the number and proportion of the three cell types associated with secretion (Paneth cell, goblet cell, enteroendocrine cell) increased (Fig. 4d). Based on this, we investigated whether the amount of substances secreted by secretory cell types (Goblet cell, Paneth cell) increased. However, there were no significant changes observed between the two groups in the levels of mucin or α-defensin produced by goblet cells and Paneth cells (Supplementary Fig. 3a, b). The genes related to substances secreted by goblet cells (*Muc2*, *Ern2*, *Agr2*, *Pdia3*) showed no significant changes between the groups, and the expression patterns of α-defensin-related genes (*Defa3*, *Defa5*, etc.) were not consistent. A similar trend was observed when examining lysozyme expression in the intestine, as IHC analysis revealed no significant difference between the two groups (Supplementary Fig. 3c, Supplementary Data 4). However, the expression of two c-type lectins, *Reg3b* and *Reg3g*, secreted by Paneth cells, was increased (Fig. 4e).

In summary, exercise reduces the expression of Wnt signaling inhibitors in ISCs, thereby influencing the activation of Wnt signaling. This, in turn, promotes the differentiation of ISCs into secretory cell types, affecting the composition of the intestinal crypt. Additionally, exercise increases the expression of c-type lectin in Paneth cells, thereby enhancing their activity.

Exercise mitigates gut barrier dysfunction seen in DIO mice in the aging model

Metabolic diseases, often driven by obesity, are known to cause various issues, including alterations in ISC function, as well as changes in cell cycle
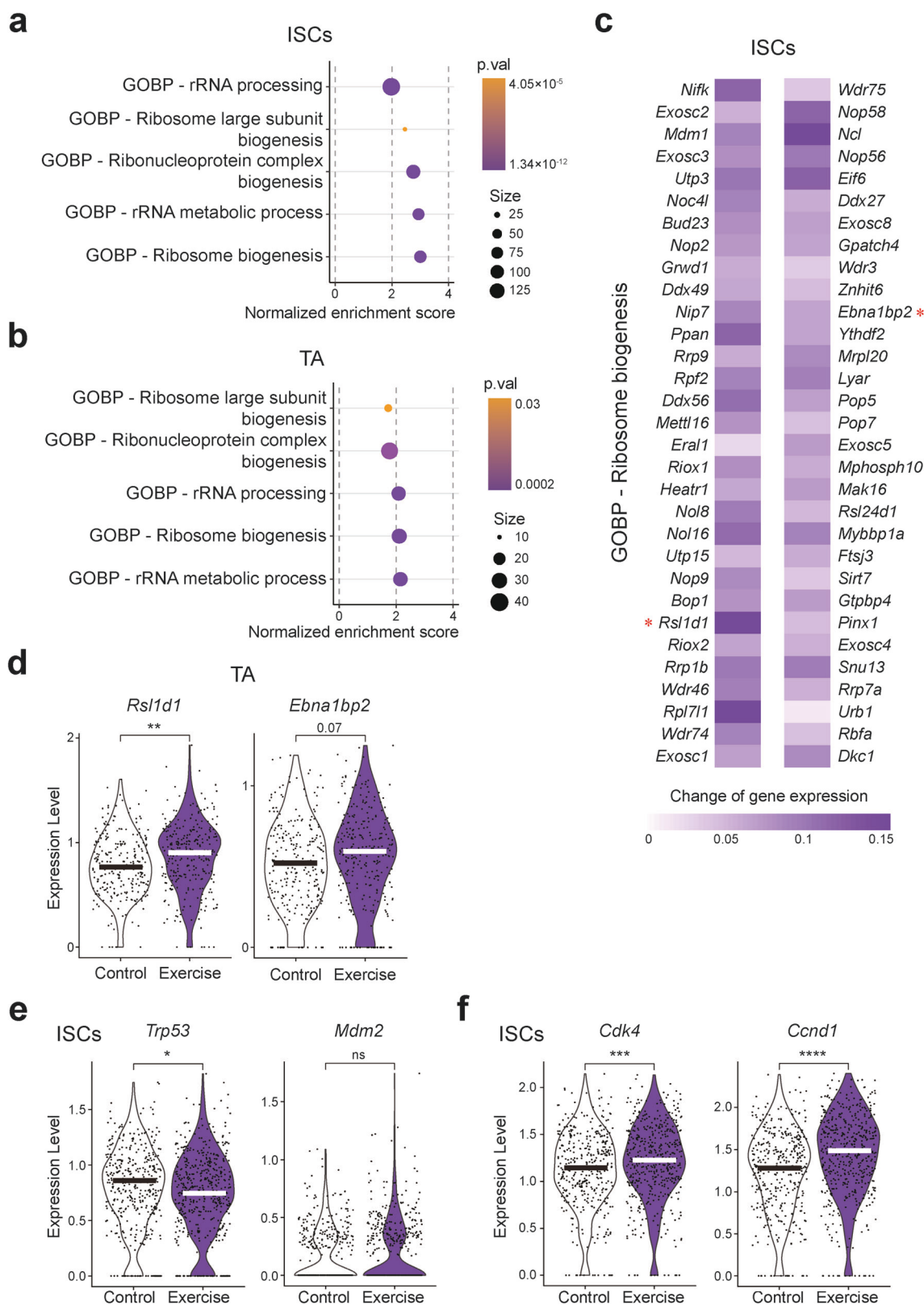
Fig. 3 | Exercise promotes ribosome biogenesis in ISCs and TA cells. a, **b** GOBP enrichment analysis in ISCs and TA from exercised mice. **c**. Differential expressions of genes involved in ribosome biogenesis in ISCs. *Rsl1d1* and *Ebna1bp2* were highlighted with red asterisks (*). **d** Expression levels of *Rsl1d1* and *Ebna1bp2* in the exercise group compared to controls in TA cell. The log(fold change) (log(FC)) values of the listed genes are greater than or equal to 0.2. **e**, **f** Expression levels of

Trp53, *Mdm2*, *Cdk4*, *Ccnd1* in ISCs. The log(fold change) (log(FC)) values of the listed genes are greater than or equal to 0.2 except *Mdm2*. *p*.val = *p* value. *P* value was calculated using *t*-test. *$P < 0.05$, **$P < 0.01$, ***$P < 0.001$, ****$P < 0.0001$, ns = non-significant ($p > 0.05$). The black and white bar in the middle of the violin plot represents the mean expression level for each group.
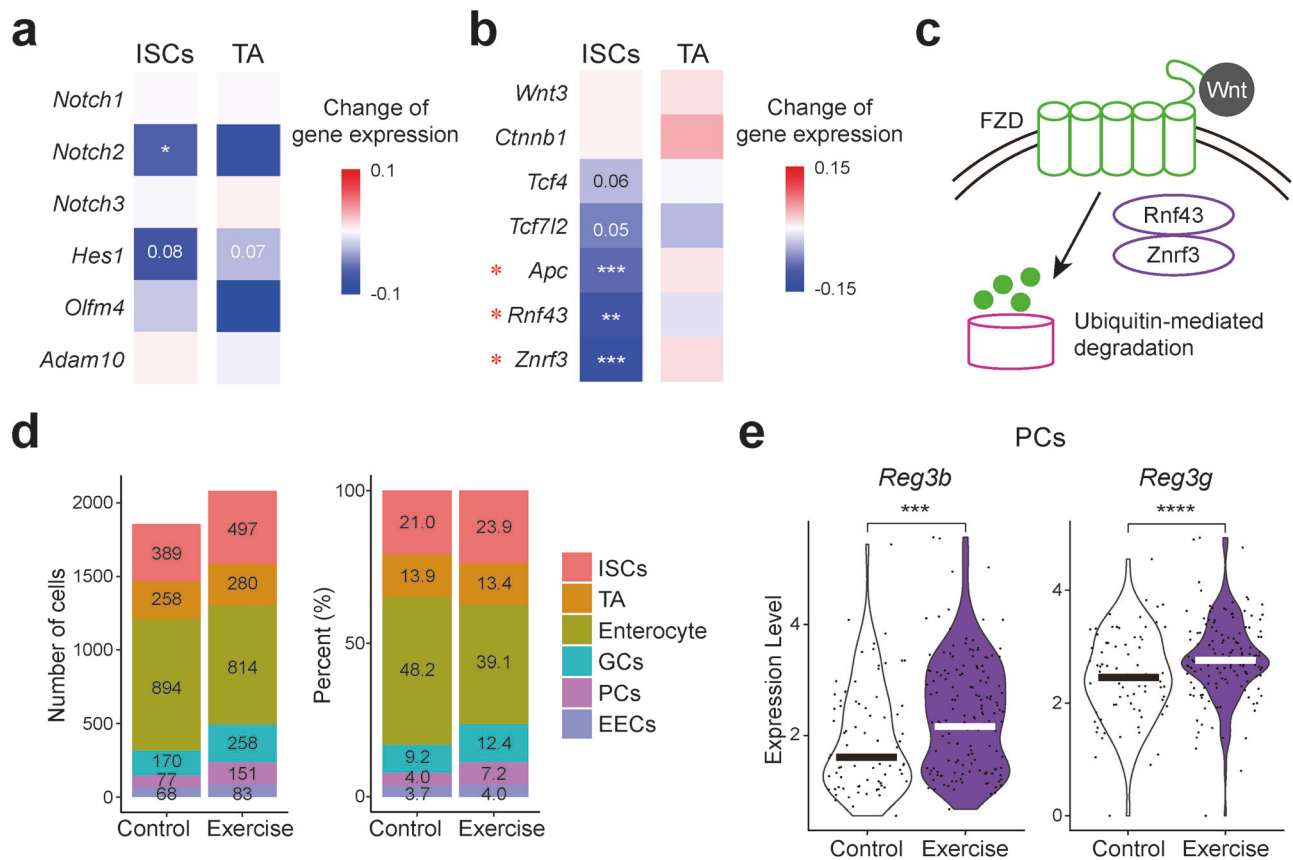
Fig. 4 | Exercise reduces the expression of Wnt signaling inhibitors, impacting intestinal homeostasis. a, b Differential expression of genes involved in the Notch and Wnt signaling pathway in ISC and TA cells in exercised mice compared with controls. The value and symbols (*, **) inside the plot represent the *p* value between the two groups. Values nonspecifically marked indicate non-significant differences. The factors that inhibit Wnt signaling were marked with red asterisks (*). **c** Schematic representation of the Wnt signaling pathway, highlighting the roles of *Rnf43* and *Znrf3* in the ubiquitin-mediated degradation of Wnt receptors. **d** The number and percentage of different cell types within the intestinal crypts in control and exercise group. The numbers inside the plot represent actual values. **e** Expression of c-type lectins in PCs. The log(fold change) (log(FC)) values of the listed genes are greater than or equal to 0.2. *P* value was calculated using *t*-test. *P < 0.05, **P < 0.01, ***P < 0.001, ****P < 0.0001. The black and white bar in the middle of the violin plot represents the mean expression level for each group.

and lipid metabolism[14,57]. To investigate whether factors observed in diet-induced obese (DIO) mice are improved in the exercise group, we compared our analysis results with publicly available data (GSE147319)[14]. This dataset consists of crypts from the whole small intestine of 3 mice fed a chow diet (CD) and 3 mice fed a high-fat diet (HFD). After quality control, a total of 27,684 cells were analyzed. 6 cell types, including Tuft cells, were annotated for each cluster (Fig. 5a). On average, each cell expressed 3500 genes (Fig. 5b). The cluster annotations were performed using the same marker gene set as in the previous analysis, with tuft cells being further classified based on the expression of 2 additional genes (*Trpm5*, *Dclk1*) (Fig. 5c).

First, we focused on the fact that obesity leads to defects in Paneth cells[12,13]. Specifically, it has been reported that in obese mice, the expression of *Reg3g* is reduced in Paneth cells[58]. When comparing the DIO mouse group with the CD mouse group, the expression of genes related to α-defensin (*Defa3*, *Defa5*, etc.) in Paneth cells showed non-significant change (Fig. 5d). However, Reg3g was reduced in the DIO mouse group as previously reported (Fig. 5e). Given the emerging role of Reg3g in alleviating metabolic dysfunction including glucose tolerance, the increase in Reg3g observed with exercise suggests that it may play a mechanistic role in improving metabolic dysfunction of intestine[58].

It is known that obesity affects gut permeability and weakens gut barrier function, leading to a phenomenon known as gut leakage[10,59]. This is also evident at the single-cell RNA sequencing level, where GSEA (Gene Set Enrichment Analysis) revealed a decrease in enterocyte cell junction organization in the DIO mouse group (p value < 0.03, Normalized enrichment score < −1.5), with reduced expression of occludin (*Ocln*), claudin (*Cldn2*),

and tight junction proteins (*Tjp3*)[11,60] (Fig. 5f). Conversely, in the exercise group, cell-cell junction organization was increased (p value < 0.04, Normalized enrichment score > 1.5). Unlike in obesity, the expression of genes including occluding and claudin (*Cldn3*) was elevated (Fig. 5g). These findings suggest that exercise improves gut barrier function, primarily by enhancing the expression of occludin.

However, other results observed in Figs. 3 and 4 did not show a consistent correlation in the intestines of the DIO mouse model. While the proportion of ISCs in the intestinal crypt significantly decreased, the proportions of TA cells and Paneth cells increased, leading to a lack of consistency (Supplementary Fig. 4a). Similarly, the Notch and Wnt signaling pathways, which influence the direction of ISCs differentiation, showed inconsistent patterns. The expression of *Hes1*, a positive regulator of Notch signaling, decreased in the ISCs and TA cells of DIO mice. Similarly, the expression of *Notch1-3* also declined, indicating that Notch signaling is reduced in these cells (Supplementary Fig. 4b). In the case of Wnt signaling, the expression of inhibitory factors decreased in ISCs and TA cells, but the expression of Wnt signaling target molecules also decreased, again leading to a lack of consistency (Supplementary Fig. 4c). Thus, the changes in signaling pathways that influence ISCs differentiation due to exercise do not appear to be correlated with those observed in DIO mice. The gene expression related to ribosome biogenesis also did not appear to be linked to exercise. In DIO mice, compared to CD-fed mice, the expression of *Rsl1d1* and *Ebna1bp2* was increased in ISCs and TA cell (Supplementary Fig. 4d, e). While the expression of *Trp53* also showed an increase, *Cdk4* and *Ccnd1* exhibited a slight upward trend, making it
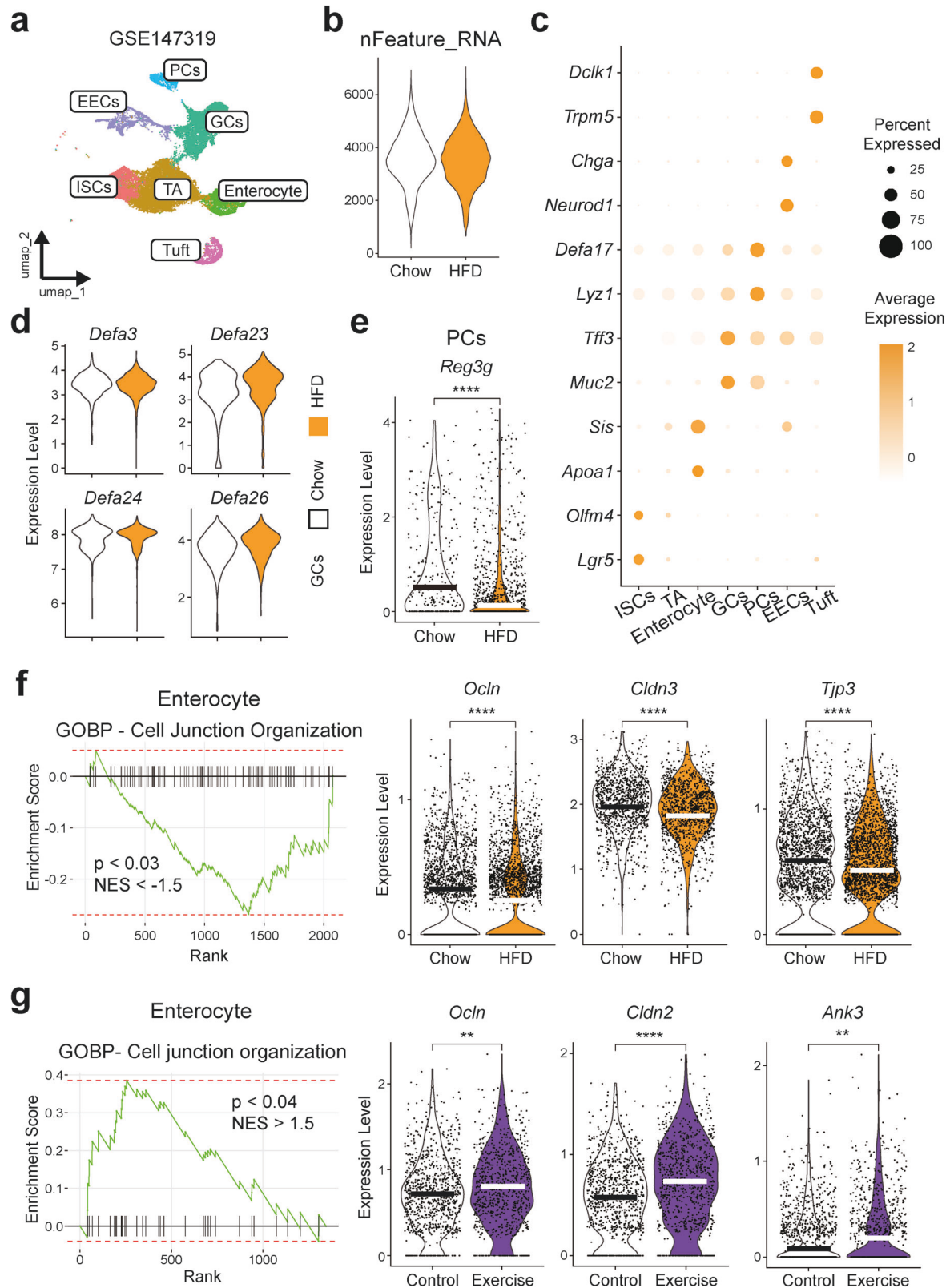
Fig. 5 | Exercise enhances metabolic homeostasis in intestinal crypts: A comparison with HFD-induced changes. a UMAP depicting the clustering of cell types within the intestinal crypt from GSE147319. **b** nFeature_RNA in crypt cells from CD and HFD-fed mice. **c** Expression levels and percentage of expression of key marker genes across the identified cell types, used for annotation. **d** Expression of α-defensin-related genes in the HFD-fed group compared to the CD-fed group. **e** Expression of *Reg3g* on PCs. The log(fold change) (log(FC)) values of the listed genes are greater than or equal to 0.2. **f, g** GSEA of enterocytes from HFD-fed and exercise group and expression of related genes. The log(fold change) (log(FC)) values of the listed genes are greater than or equal to 0.2. *P* value was calculated using *t*-test. **$P < 0.01$, ****$P < 0.0001$. *P* = p value, NES = Normalized enrichment score. The black and white bar in the middle of the violin plot represents the mean expression level for each group.
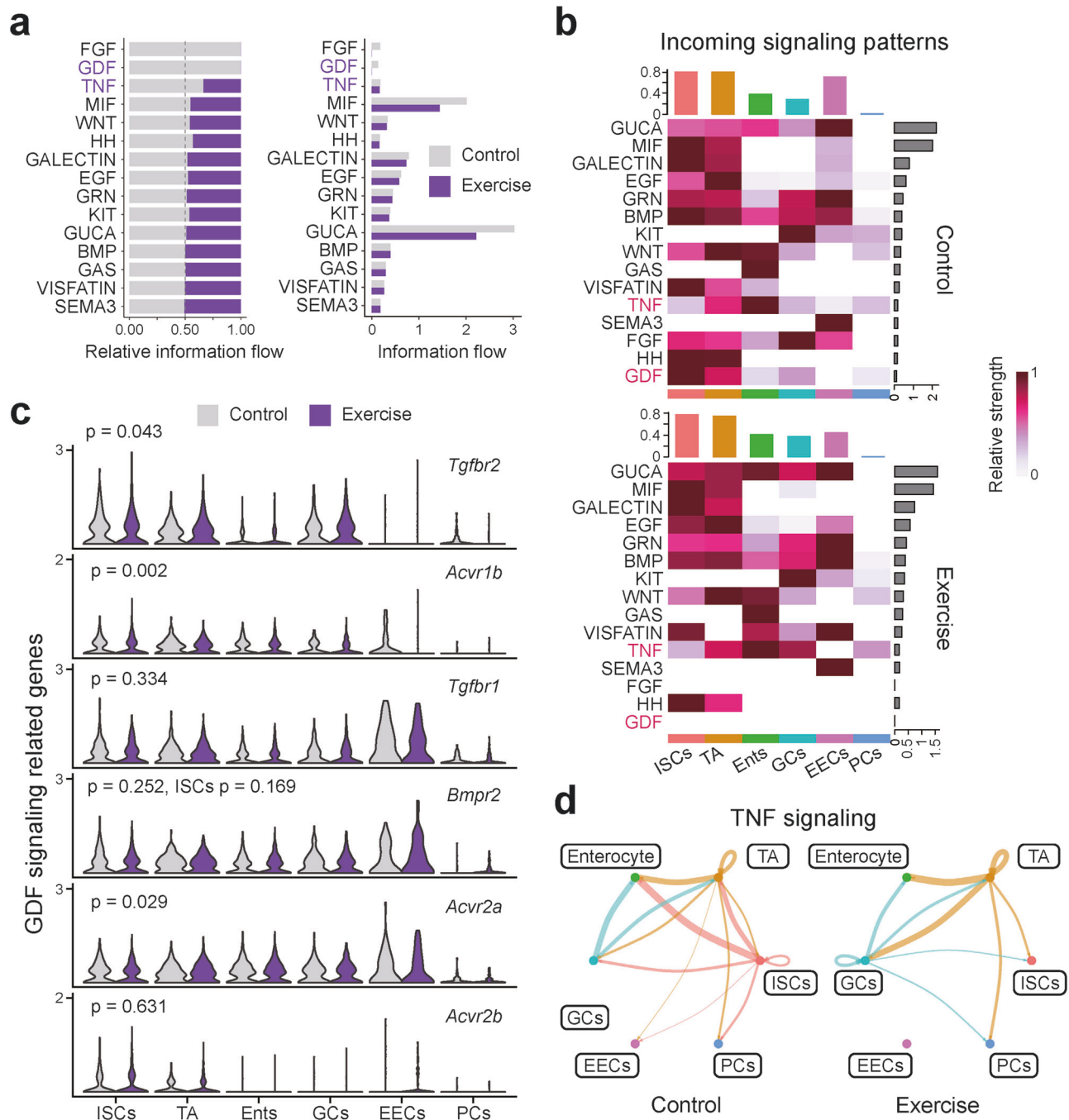
Fig. 6 | GDF and TNF signaling are reduced in exercise mice. a The information flows between the two groups. Left displays the relative proportion changes between the two groups, Right shows the absolute changes in the signaling pathway. **b** The incoming signaling pattern between the control and exercise group. **c** Expression of receptor of GDF signaling. *P* value was calculated using *t*-test and based on the comparison between the two groups across the entire intestinal crypt. **d** Levels of cell-cell communication for TNF signaling.

difficult to establish consistency in the expression of senescence marker genes (Supplementary Fig. 4f, g). In summary, there seems to be no correlation between signaling pathways or ribosome biogenesis when comparing DIO mice with exercised mice.

Exercise reduces GDF and TNF signaling pathways, improving senescence profile

In the intestinal crypt, aside from previously examined signaling pathways, there may be additional pathways influenced by external factors. To investigate this, we utilized the CellChat package to analyze the incoming

signaling pathways between the exercised and control group[61]. Initially, we assessed the overall number and strength of interactions and found no significant differences; however, in the exercised group, both the number of inferred interactions and their strength were reduced (Supplementary Fig. 5a). When comparing specific signaling pathways between the two groups, we observed that while there were no major differences overall, the GDF and TNF signaling pathways were relatively decreased (Purple) (Fig. 6a). Additionally, when comparing the enrichment of incoming signaling pathways across the intestinal crypt, these two pathways showed noticeable changes (Red) (Fig. 6b).

GDF (Growth Developmental Factor) signaling is a pathway influenced by the TGF-β superfamily, with GDF11 and GDF15 previously known to impact aging[62–64]. However, the changes observed in the intestine do not appear to be directly caused by decrease in GDF11 and GDF15. When examining the expression of genes involved in GDF signaling across different cell types, the expression of *Gdf11* and *Gdf15* was hardly observed (Supplementary Fig. 5b). Instead, a decrease in the expression of genes related to GDF signaling receptors (*Tgfbr2*, *Acvr1b*, *Bmpr2*, *Acvr2a*) was noted (Fig. 6c). This is consistent with the previously observed reduction in the incoming pattern of GDF signaling (Fig. 6B). Similarly, the incoming signaling pattern of TNF signaling was also observed to decrease. Notably, while the overall incoming pattern decreased, there was a significant reduction in cell-cell communication within the pathway, especially in ISCs (Fig. 6d). When examining gene expression changes, while the decrease in *Tnf* between the two groups was not statistically significant ($p = 0.077$), its receptor *Tnfrsf1a* showed a significant reduction in the exercise group (Supplementary Fig. 5c). Although the impact of TNF signaling on senescence, cell cycle progression, and small intestine homeostasis remains controversial, previous studies have suggested that TNF signaling contributes to the inhibition of WNT signaling[65–68]. This could imply that the changes observed in WNT signaling might also be influenced by the reduction in TNF signaling. Lastly, FGF signaling also showed a decrease in both information flow and incoming signaling patterns (Fig. 6a, b). This reduction appears to be due to the decreased expression of *Fgfr2* and *Fgfr4* (Supplementary Fig. 5d) although the decrease in these two genes was not statistically significant ($p = 0.159, 0.214$).

As with the earlier observations, we examined whether cell-cell communication changed in the DIO mice model. While inferred interactions and interaction strength showed a slight increase in HFD-fed mice, the information flow analysis revealed no clear contrast when compared to the exercise-induced mouse model (Supplementary Fig. 5e, f).

Discussion

In this study, we compared the intestinal crypts of aged mice that underwent exercise with those of non-exercised aged mice to identify any differences and assess whether these differences influenced the expression of aging hallmarks. Additionally, we compared these changes with the intestinal crypts of DIO mice to determine if there were any effects on the function of intestinal cells. We observed that exercise induced cell cycle progression, with key regulatory factors also shifting towards promoting cell cycle advancement. Notably, ribosome biogenesis enrichment increased in both ISCs and TA cells. Also, the expression of *Trp53* was reduced, while the expression of *Cdk4* and *Ccnd1* was elevated. These findings suggest that exercise can alleviate cell cycle arrest and support the proliferation and function of ISCs. Additionally, exercised mice reduced the expression of Wnt signaling inhibitors like *Apc*, *Rnf43*, and *Znrf3*, thereby maintaining or promoting Wnt signaling activity, which likely contributes to the differentiation of ISCs into secretory cell types (Fig. 7). The changes in the intestine induced by exercise also showed positive improvements when compared to those observed in the intestines of obese mouse models. In Paneth cell, the level of *Reg3g*, which had decreased in the obese model, were increased in the exercise model. Furthermore, the improvements in gut barrier function, suggest that exercise may protect against the gut leakage phenomenon commonly seen in obesity and aging (Fig. 7). Lastly, the reduction in GDF signaling and TNF signaling was observed to correlate with a decrease in senescence-related signaling in ISCs.

These findings carry several important implications. First, it is necessary to investigate how the observed changes in ribosome biogenesis, and cell cycle progression in ISCs impact the intestinal crypt and, more broadly, the small intestine. If ribosome biogenesis is impaired in stem cells, it is known that they cannot function properly, and this is likely true for ISCs as well[69,70]. Considering that ISCs significantly influence the entire small intestine by interacting with the microbiome and maintaining intestinal homeostasis, it is essential to explore how these changes affect the intestine systemically. This suggests that future studies need to adopt a broader perspective to fully understand these systemic interactions. The second point concerns Reg3g, produced by Paneth cells. While Reg3g primarily functions as an anti-microbial peptide, it has also been shown to support glucose homeostasis and maintain gut barrier function following bariatric surgery[58]. Although there may not be a well-established connection between Reg3g and senescence, these findings suggest that Reg3g, induced by exercise, could contribute to maintaining gut homeostasis. The final point that warrants further exploration is the role of TNF signaling in the context of exercise and intestinal aging. While some studies suggest that TNF may inhibit Wnt signaling and thereby influence senescence, more research is needed to clarify these mechanisms[65,66].

Despite the promising finding, this study also identified several gaps that require further investigation. One notable issue is the reduction in FGF (Fibroblast growth factor) signaling observed in the exercise group (Fig. 6a, b). The FGF pathway is well-known for its role in inhibiting cellular senescence. Previous studies have shown that FGF stimulation is crucial for preventing extrinsic senescence and that FGF inhibit cellular senescence through the PI3K-AKT-MDM2 pathway[71,72]. However, the expression of key FGF signaling components such as *Fgfr2* and *Fgfr4* are downregulated in exercise group compared to control (Supplementary Fig. 2d). This finding is counterintuitive given the established role in FGFR2 and FGFR4 in preventing senescence, as demonstrated by previous studies showing that the loss of FGF receptor interaction leads to stem cell senescence, and FGFR4 inhibition can promote senescence[71,73]. These contradictory results suggest that the relationship between FGF signaling and exercise-induced effects on intestinal health may be more complex than previously understood, and further studies are needed to clarify these interactions.

This study is based on single-cell RNA sequencing, which allows us to observe key phenotypic changes, such as ISC cell cycle progression and gut barrier integrity. However, single-cell RNA sequencing alone has limitations in fully elucidating the mechanistic drivers of these changes. For instance, while our analysis suggests that exercise promotes ISCs proliferation, additional validation using EdU incorporation assays or flow cytometry would further strengthen this finding.

While our analysis revealed an increase in the proportion of secretory cell types in the exercise group, the levels of mucin and α-defensin secreted by goblet and Paneth cells did not show significant changes. It is possible that transcriptional data alone may not fully capture functional protein levels. Additional validation, such as immunohistochemical staining for markers like lysozyme and mucin, would have provided more direct evidence of changes in secretory activity. This discrepancy can be explained by multiple factors. First, post-transcriptional regulation plays a significant role in determining secretory output, meaning that increased differentiation into secretory cell types does not necessarily translate into an immediate increase in protein secretion[74]. Studies have shown that goblet cell mucin secretion is influenced by environmental cues such as microbiome interactions and inflammatory signals, rather than just cell number[75]. Similarly, Paneth cell defensin production is tightly regulated at the translational and post-translational levels through factors like bacterial interaction[76]. Furthermore, exercise may prioritize epithelial maintenance over immediate secretion, influencing energy allocation and mucosal homeostasis[77]. Finally, alternative protective mechanisms, such as increased expression of C-type lectins (Reg3b, Reg3g), may compensate for the lack of significant changes in mucin and α-defensin levels. Taken together, these findings suggest that while exercise promotes intestinal secretory cell differentiation, additional factors regulate the actual levels of mucins and antimicrobial peptides, requiring further investigation into post-transcriptional regulation and functional assays.

The close relationship between obesity and gut health is well established. Previous studies have consistently reported that gut barrier integrity is compromised in various metabolic disease mouse models, including diet-induced obesity (DIO) mice and ob/ob mice, when compared to healthy controls[11]. In this study, we demonstrated that exercise can improve gut barrier integrity, specifically by upregulating genes related to tight junction proteins, such as claudin and occludin. Similarly, although we leveraged
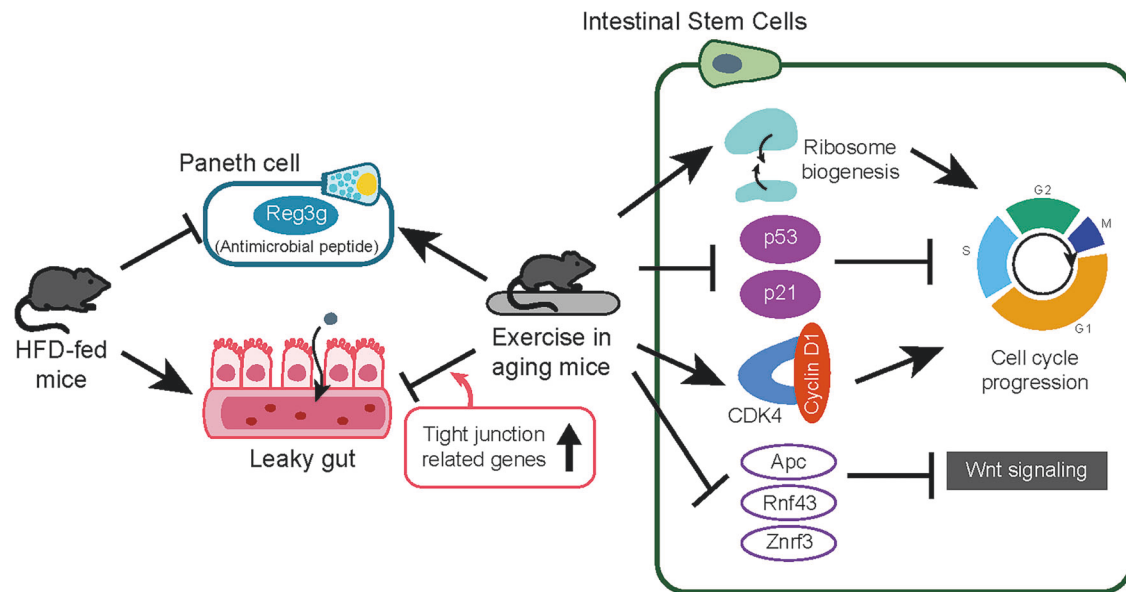
Fig. 7 | Regular exercise helps maintain the homeostasis of the small intestine.

public datasets from DIO mice to explore the relationship between exercise, gut barrier function, and Reg3 family proteins in aging, the inherent limitations of public datasets prevent direct one-to-one comparisons with our experimental data. For a more accurate comparison, it would be necessary to analyze mice experiencing both aging and obesity simultaneously, along with an exercise group under the same conditions.

To gain deeper mechanistic insights, further wet-lab experiments, such as Western blotting, flow cytometry, and genetic or pharmacological inhibition studies, will be necessary. Additionally, due to experimental constraints, the number of mice used in this study was limited. Future in vivo studies with larger sample sizes will be essential to validate these findings more robustly.

In conclusion, this study underscores the significant role of exercise in modulating key cellular processes within the intestinal crypts, particularly those involved in cell cycle, ribosome biogenesis, and Wnt signaling. Notably, compared to the obese phenotype, we observed an increase in Reg3g expression and an improvement in gut integrity in the exercised group. These findings contribute to understanding of how regular physical activity can influence intestinal health and suggest potential mechanisms through which exercise may delay the aging process and prevent age-associated intestinal disorders.

Methods
Mouse
22-month-old male C57BL/6J mice were housed in climate-controlled, specific pathogen-free barrier facilities under a 12-h light-dark cycle. Mice were randomly divided into training ($n = 6$) and control ($n = 6$) and maintained on a normal chow diet. To reduce the environmental variation, both groups were moved within the same environment during the exercise period. At the end of the experiment, all mice were euthanized by CO_2 inhalation in a dedicated chamber following institutional animal care guidelines. No animal or data points were excluded during the experiment or data analysis. All animals completed the full exercise protocol and were included in the results. All experimental protocols were approved by the Institutional Animal Care and Use Committee of the Gwangju Institute of Science and Technology (No. GIST-2021-101).

Exercise
The training group performed running exercises using a treadmill 3 times per week for the entire experimental period. Before each exercise, the mice underwent a one-minute incubation in the treadmill machine to facilitate

adaptation. The mice performed exercising using a treadmill speed was set at 5 m/min, with increments of 5 m/min every 5 min, reaching a final speed of 25 m/min over a total duration of 25 min. To prevent exercise adaptation in the mice, during the second 4 weeks, the initial treadmill speed was set at 5.6 m/min, with increments of 5.6 m/min every 5 min, reaching a final speed of 28 m/min. All treadmill exercises were conducted at an incline of 5 degrees, with electrical stimulation applied at 0.15 mA. The control group was exposed to the same environment during the exercise training but did not perform physical activity, to eliminate environmental effects.

Power and endurance test
The day before the test, a warm-up was conducted to allow the mice to become accustomed to the treadmill machine. Before initiating the warm-up, the mice underwent a one-minute incubation in the treadmill machine to facilitate adaptation. The warm-up was conducted at a speed of 15 m/min for a duration of 5 min. In the power test, the initial speed was set at 10.8 m/min and the speed was increased by 1.2 m/min per minute. During the endurance test, the starting speed was 10.8 m/min, with increments of 1.8 m/min every 12 min. Both the power test and the endurance test measured the time to exhaustion. All treadmill exercises were conducted at an incline of 5 degrees, with electrical stimulation applied at 0.15 mA.

Immunohistochemistry (IHC)
After sacrificing the mice, the ileum was separated and immediately stored in 10% formalin (F2013, Biosesang). The production of paraffin blocks and IHC slides ($n = 4$) was carried out by KPNT (Cheongju-si, Chungcheongbuk-do, Republic of Korea), following their standardized protocol. Antibody was used A0262 (ABclonal) for p16INK4a, PA1-30399 (Invitrogen) for p21, ab2893 (Abcam) for γ-H2AX, and MA5-32154 (Invitrogen) for lysozyme. Two tissue sections were taken from each specimen to create replicates. At 4× (p16INK4a, p21, γ-H2AX, lysozyme) or 20× (p21) magnification, two random images were captured. The captured images were analyzed using ImageJ (ij153-win-java8). First, to measure the area occupied by the tissue, an RGB stack was generated, and the Threshold value was set to distinguish the tissue from the background. Next, to quantify the antibody-stained area, the original image was converted to an HSB stack, and the Threshold value was set to reflect staining intensity. Finally, the stained area was normalized to the total tissue area to calculate the p21 area (IHC area).

Intestinal crypt isolation

Ileum is trimmed and cut into half to open the ring-shaped tube. Minced ileum is incubated in 5 ml of 20 mM EDTA-PBS solution, 4 °C for 90 min. The solution is vortexed for 10 s every 30 minutes, and the solution is replaced with fresh one. Apply crypt dissociated solution under microscopy to check proportion of villi and crypts. Collect solutions with high portion of crypt and centrifuge for $300 \times g$, 3 min, 4 °C. Collect the pellets and apply 3 ml of TrypLE for 10 min. Pass the digested crypt through 100 μm filter and wash with cold PBS for three times. Resuspend the crypt cells into 0.2% BSA-PBS solution for further application.

Single cell RNA sequencing

Single-cell sequencing was performed using the Seurat package (5.0.3) in R. We filtered out cells with an nFeature_RNA > 500 and used them for analysis. The "FindVariableFeatures()" function with the vst method was used to select highly variable genes based on their expression levels (nfeatures = 3000). Annotation of clusters was performed by visually inspecting the expression of marker genes for each cell type using the "DotPlot()" function. Marker genes were selected based on previous studies or by referring to data available in PanglaoDB (https://panglaodb.se/search.html). The identification of DEGs (Differentially expressed genes) was conducted using the "FindMarkers()" function. Log fold change (log(FC)) threshold of 0.2 was set, and only DEGs with a p value below 0.05 were considered for analysis. Public dataset GSE147319 was preprocessed using the scanpy toolkit in Python. Subsequently, the rhdf5 (2.42.0) package and SeuratDisk (0.0.0.9020) package were utilized to transform the data into a Seurat object, enabling further analysis. Annotation of clusters was performed using the genes utilized in the reference study of this dataset. "FeaturePlot()" function was used to visually confirm the expression patterns of these genes within the clusters. Identification of DEGs was conducted using "FindMarkers()". log(FC) threshold of 0.2 was set, and only DEGs with a p value below 0.05 were considered for analysis.

The gene list of SenMayo was directly downloaded from GSEA (https://www.gsea-msigdb.org/gsea/msigdb/human/geneset/SAUL_SEN_MAYO.html) and applied to our dataset. Using the same method employed for the subsequent pathway analysis, we represented the enrichment of exercised group compared to control group using an enrichment plot.

Cell cycle scoring was conducted by referring to the cell cycle scoring vignette included in the Seurat package. Using the "CellCycleScoring()" function, we examined which phase (S phase or G2/M phase) the cells in each group were in, based on the associated genes.

Gene expression comparisons were visualized using violin plots and heatmaps. The Seurat package's "VlnPlot()" function was used to compare the level of gene expression between the two groups. Additionally, the "geom_boxplot()" function was utilized to display the position of the mean within the violin plot for clearer interpretation. To visualize gene expression using heatmaps, we first extracted the expression levels of genes related to Notch and Wnt signaling using the "AverageExpression()" function. We then calculated the difference between the average expression in the Exercise (or HFD) group and the control (or CD) group. The smallest and largest values among these differences were set as the breaks for the heatmap, which was then used to represent the expression differences visually.

Pathway analysis

For the PROGENy (1.20.0), we first performed "progeny()" on the top 1000 genes. We then divided the range between the minimum and maximum "progeny score" into 100 intervals to create breaks. These breaks were used to generate a heatmap, visually representing the progeny scores.

GSEA was conducted using the clusterProfiler (4.6.0), DOSE (3.24.2), msigdbr (7.5.1), fgsea (1.24.0) packages. The GOBP dataset (m5.go.bp.v2022.1.Mm.symbols.gmt) from the GSEA website was used as the database. DEGs were identified using Seurat's "FindMarkers()" function. The "fgseaMultilevel()" function was then employed to assess pathway enrichment, with a p value below 0.05 considered indicative of significant enrichment changes. The enrichment plots were visualized using the "plotEnrichment()" function.

CellChat analysis was performed using the CellChat (1.6.1) package. During the "computeCommunProb()" process, the "type" parameter was set to "triMean", and communication filtering was configured to require a minimum of 5 cells (min.cells = 5) per communication.

Statistical analysis

The p values for in vivo data, such as body weight, power and endurance tests, as well as the IHC area, were calculated using GraphPad. P values for the comparison of gene expression levels in the single-cell dataset were calculated using the ggpubr (0.5.0). Cross-validation was performed using the "FindMarkers()" function in the Seurat package. The method used to calculate each p value is specified in the respective figure legends. In the pathway analysis, P values were calculated using values obtained from the clusterProfiler, and fgsea packages.

Data availability

The datasets used and/or analyzed during the current study are available from the corresponding author on reasonable request.

Code availability

The underlying code for this study is not publicly available but may be made available to qualified researchers on reasonable requests from the corresponding author.

References

1. Joyner, M. J. & Green, D. J. Exercise protects the cardiovascular system: effects beyond traditional risk factors. *J. Physiol.* **587**, 5551–5558 (2009).
2. Seals, D. R., Justice, J. N. & LaRocca, T. J. Physiological geroscience: targeting function to increase healthspan and achieve optimal longevity. *J. Physiol.* **594**, 2001–2024 (2016).
3. Lakka, T. A. & Laaksonen, D. E. Physical activity in prevention and treatment of the metabolic syndrome. *Appl. Physiol. Nutr. Metab.* **32**, 76–88 (2007).
4. Bonomini, F., Rodella, L. F. & Rezzani, R. Metabolic syndrome, aging and involvement of oxidative stress. *Aging Dis.* **6**, 109–120 (2015).
5. Salvestrini, V., Sell, C. & Lorenzini, A. Obesity may accelerate the aging process. *Front. Endocrinol.* **10,** https://doi.org/10.3389/fendo.2019.00266 (2019).
6. Ahima, R. S. Connecting obesity, aging and diabetes. *Nat. Med.* **15**, 996–997 (2009).
7. Kohrt, W. M. et al. Insulin resistance in aging is related to abdominal obesity. *Diabetes* **42**, 273–281 (1993).
8. Fasano, A. & Shea-Donohue, T. Mechanisms of disease: the role of intestinal barrier function in the pathogenesis of gastrointestinal autoimmune diseases. *Nat. Clin. Pract. Gastroenterol. Hepatol.* **2**, 416–422 (2005).
9. Lin, L. & Zhang, J. Role of intestinal microbiota and metabolites on gut homeostasis and human diseases. *BMC Immunol.* **18**, 2 (2017).
10. Teixeira, T. F. S., Collado, M. C., Ferreira, C. L. L. F., Bressan, J. & Peluzio, M.dC. G. Potential mechanisms for the emerging link between obesity and increased intestinal permeability. *Nutr. Res.* **32**, 637–647 (2012).
11. Brun, P. et al. Increased intestinal permeability in obese mice: new evidence in the pathogenesis of nonalcoholic steatohepatitis. *Am. J. Physiol.-Gastrointest. Liver Physiol.* **292**, G518–G525 (2007).
12. Hodin, C. M. et al. Reduced Paneth cell antimicrobial protein levels correlate with activation of the unfolded protein response in the gut of obese individuals. *J. Pathol.* **225**, 276–284 (2011).

13. Liu, T.-C. et al. Western diet induces Paneth cell defects through microbiome alterations and farnesoid X receptor and type I interferon activation. *Cell Host Microbe* **29**, 988–1001.e1006 (2021).

14. Aliluev, A. et al. Diet-induced alteration of intestinal stem cell function underlies obesity and prediabetes in mice. *Nat. Metab.* **3**, 1202–1216 (2021).

15. López-Otín, C., Blasco, M. A., Partridge, L., Serrano, M. & Kroemer, G. The Hallmarks of aging. *Cell* **153**, 1194–1217 (2013).

16. Brogna, A., Ferrara, R., Bucceri, A. M., Lanteri, E. & Catalano, F. Influence of aging on gastrointestinal transit time: an ultrasonographic and radiologic study. *Investig. Radiol.* **34**, 357 (1999).

17. Myers, J. Exercise and cardiovascular health. *Circulation* **107**, e2–e5 (2003).

18. Schafer, M. J. et al. Exercise prevents diet-induced cellular senescence in adipose tissue. *Diabetes* **65**, 1606–1615 (2016).

19. Ahlskog, J. E., Geda, Y. E., Graff-Radford, N. R. & Petersen, R. C. Physical exercise as a preventive or disease-modifying treatment of dementia and brain aging. *Mayo Clin. Proc.* **86**, 876–884 (2011).

20. Gehart, H. & Clevers, H. Tales from the crypt: new insights into intestinal stem cells. *Nat. Rev. Gastroenterol. Hepatol.* **16**, 19–34 (2019).

21. Snippert, H. J. et al. Intestinal crypt homeostasis results from neutral competition between symmetrically dividing Lgr5 stem cells. *Cell* **143**, 134–144 (2010).

22. Clevers, H. The intestinal crypt, a prototype stem cell compartment. *Cell* **154**, 274–284 (2013).

23. Nalapareddy, K. et al. Canonical Wnt signaling ameliorates aging of intestinal stem cells. *Cell Rep.* **18**, 2608–2621 (2017).

24. Minafra, L., Bravatà, V., Cammarata, F., Di Maggio, F. & Forte, G. SASPects of radiation induced senescence. *Ann. Radiat. Ther. Oncol.* **1**, 1006 (2017).

25. Li, T. et al. Tumor suppression in the absence of p53-mediated cell-cycle arrest, apoptosis, and senescence. *Cell* **149**, 1269–1283 (2012).

26. Saito, Y., Yamamoto, S. & Chikenji, T. S. Role of cellular senescence in inflammation and regeneration. *Inflamm. Regen.* **44**, 28 (2024).

27. Ren, J. L., Pan, J. S., Lu, Y. P., Sun, P. & Han, J. Inflammatory signaling and cellular senescence. *Cell Signal.* **21**, 378–383 (2009).

28. Saltiel, A. R. & Olefsky, J. M. Inflammatory mechanisms linking obesity and metabolic disease. *J. Clin. Investig.* **127**, 1–4 (2017).

29. Li, X. et al. Inflammation and aging: signaling pathways and intervention therapies. *Signal Transduct. Target. Ther.* **8**, 239 (2023).

30. Gorgoulis, V. et al. Cellular senescence: defining a path forward. *Cell* **179**, 813–827 (2019).

31. Herranz, N. & Gil, J. Mechanisms and functions of cellular senescence. *J. Clin. Invest* **128**, 1238–1246 (2018).

32. Demitrack, E. S. & Samuelson, L. C. Notch regulation of gastrointestinal stem cells. *J. Physiol.* **594**, 4791–4803 (2016).

33. Mah, A. T., Yan, K. S. & Kuo, C. J. Wnt pathway regulation of intestinal stem cells. *J. Physiol.* **594**, 4837–4847 (2016).

34. Tian, H. et al. Opposing Activities of Notch and Wnt Signaling Regulate Intestinal Stem Cells and Gut Homeostasis. *Cell Rep.* **11**, 33–42 (2015).

35. Suzuki, K. et al. Hes1-deficient mice show precocious differentiation of Paneth cells in the small intestine. *Biochem. Biophys. Res. Commun.* **328**, 348–352 (2005).

36. Scoville, D. H., Sato, T., He, X. C. & Li, L. Current view: intestinal stem cells and signaling. *Gastroenterology* **134**, 849–864 (2008).

37. Schultz, M. B. & Sinclair, D. A. When stem cells grow old: phenotypes and mechanisms of stem cell aging. *Development* **143**, 3–14 (2016).

38. Saul, D. et al. A new gene set identifies senescent cells and predicts senescence-associated pathways across tissues. *Nat. Commun.* **13**, 4827 (2022).

39. Schubert, M. et al. Perturbation-response genes reveal signaling footprints in cancer gene expression. *Nat. Commun.* **9**, 20 (2018).

40. Yosef, R. et al. p21 maintains senescent cell viability under persistent DNA damage response by restraining JNK and caspase signaling. *EMBO J.* **36**, 2280–2295 (2017).

41. Mah, L. J., El-Osta, A. & Karagiannis, T. C. γH2AX: a sensitive molecular marker of DNA damage and repair. *Leukemia* **24**, 679–686 (2010).

42. Lessard, F. et al. Senescence-associated ribosome biogenesis defects contributes to cell cycle arrest through the Rb pathway. *Nat. Cell Biol.* **20**, 789–799 (2018).

43. Nishimura, K. et al. Perturbation of ribosome biogenesis drives cells into senescence through 5S RNP-mediated p53 activation. *Cell Rep.* **10**, 1310–1323 (2015).

44. Dörner, K., Ruggeri, C., Zemp, I. & Kutay, U. Ribosome biogenesis factors—from names to functions. *EMBO J.* **42**, e112699 (2023).

45. Mende, N. et al. CCND1–CDK4–mediated cell cycle progression provides a competitive advantage for human hematopoietic stem cells in vivo. *J. Exp. Med.* **212**, 1171–1183 (2015).

46. Rader, J. et al. Dual CDK4/CDK6 inhibition induces cell-cycle arrest and senescence in neuroblastoma. *Clin. Cancer Res.* **19**, 6173–6182 (2013).

47. Del Toro, N. et al. Ribosomal protein RPL22/eL22 regulates the cell cycle by acting as an inhibitor of the CDK4-cyclin D complex. *Cell Cycle* **18**, 759–770 (2019).

48. Mijit, M., Caracciolo, V., Melillo, A., Amicarelli, F. & Giordano, A. Role of p53 in the regulation of cellular senescence. *Biomolecules* **10**, https://doi.org/10.3390/biom10030420 (2020).

49. Umar, S. Intestinal stem cells. *Curr. Gastroenterol. Rep.* **12**, 340–348 (2010).

50. Sanman, L. E. et al. Transit-amplifying cells coordinate changes in intestinal epithelial cell-type composition. *Dev. cell* **56**, 356–365.e359 (2021).

51. Wu, D. & Prives, C. Relevance of the p53–MDM2 axis to aging. *Cell Death Differ.* **25**, 169–179 (2018).

52. Gannon, H. S., Donehower, L. A., Lyle, S. & Jones, S. N. Mdm2–p53 signaling regulates epidermal stem cell senescence and premature aging phenotypes in mouse skin. *Devel. Biol.* **353**, 1–9 (2011).

53. Hankey, W., Frankel, W. L. & Groden, J. Functions of the APC tumor suppressor protein dependent and independent of canonical WNT signaling: implications for therapeutic targeting. *Cancer Metastasis Rev.* **37**, 159–172 (2018).

54. Katoh, M. & Katoh, M. WNT signaling pathway and stem cell signaling network. *Clin. Cancer Res.* **13**, 4042–4045 (2007).

55. Koo, B.-K. et al. Tumour suppressor RNF43 is a stem-cell E3 ligase that induces endocytosis of Wnt receptors. *Nature* **488**, 665–669 (2012).

56. Hao, H.-X. et al. ZNRF3 promotes Wnt receptor turnover in an R-spondin-sensitive manner. *Nature* **485**, 195–200 (2012).

57. de Wit, N. J. W. et al. The role of the small intestine in the development of dietary fat-induced obesity and insulin resistance in C57BL/6J mice. *BMC Med. Genom.* **1**, 14 (2008).

58. Shin, J. H. et al. The gut peptide Reg3g links the small intestine microbiome to the regulation of energy balance, glucose levels, and gut function. *Cell Metab.* **34**, 1765–1778.e1766 (2022).

59. Shemtov, S. J. et al. The intestinal immune system and gut barrier function in obesity and ageing. *FEBS J.* **290**, 4163–4186 (2023).

60. Ahmad, R., Rah, B., Bastola, D., Dhawan, P. & Singh, A. B. Obesity-induces organ and tissue specific tight junction restructuring and barrier deregulation by claudin switching. *Sci. Rep.* **7**, 5125 (2017).

61. Jin, S. et al. Inference and analysis of cell-cell communication using CellChat. *Nat. Commun.* **12**, 1088 (2021).

62. Egerman, M. A. & Glass, D. J. The role of GDF11 in aging and skeletal muscle, cardiac and bone homeostasis. *Crit. Rev. Biochem. Mol. Biol.* **54**, 174–183 (2019).

63. Liu, H. et al. GDF15 as a biomarker of ageing. *Exp. Gerontol.* **146**, 111228 (2021).

64. Conte, M. et al. GDF15, an emerging key player in human aging. *Ageing Res. Rev.* **75**, 101569 (2022).

65. Jacobson, E. C. et al. TNF-α differentially regulates cell cycle genes in promyelocytic and granulocytic HL-60/S4 cells. *G3* **9**, 2775–2786 (2019).

66. Song, K. et al. Tumor necrosis factor–related apoptosis-inducing ligand (TRAIL) is an inhibitor of autoimmune inflammation and cell cycle progression. *J. Exp. Med.* **191**, 1095–1104 (2000).

67. Li, P. et al. The inflammatory cytokine TNF-α promotes the premature senescence of rat nucleus pulposus cells via the PI3K/Akt signaling pathway. *Sci. Rep.* **7**, 42938 (2017).

68. Fafilek, B. et al. Troy, a tumor necrosis factor receptor family member, interacts with Lgr5 to inhibit Wnt signaling in intestinal stem cells. *Gastroenterology* **144**, 381–391 (2013).

69. Sharifi, S., da Costa, H. F. R. & Bierhoff, H. The circuitry between ribosome biogenesis and translation in stem cell function and ageing. *Mech. Ageing Dev.* **189**, 111282 (2020).

70. Sanchez, C. arlosG. et al. Regulation of ribosome biogenesis and protein synthesis controls germline stem cell differentiation. *Cell Stem Cell* **18**, 276–290 (2016).

71. Coutu, D. L., François, M. & Galipeau, J. Inhibition of cellular senescence by developmentally regulated FGF receptors in mesenchymal stem cells. *Blood* **117**, 6801–6812 (2011).

72. Coutu, D. L. & Galipeau, J. Roles of FGF signaling in stem cell self-renewal, senescence and aging. *Aging* **3**, 920–933 (2011).

73. Sasaki, N. et al. FGFR4 inhibitor BLU9931 attenuates pancreatic cancer cell proliferation and invasion while inducing senescence: evidence for senolytic therapy potential in pancreatic cancer. *Cancers* **12**, 2976 (2020).

74. Gregorieff, A. et al. The ets-domain transcription factor Spdef promotes maturation of goblet and paneth cells in the intestinal epithelium. *Gastroenterology* **137**, 1333–1345.e1333 (2009).

75. Johansson, M. E. V., Larsson, J. M. H. & Hansson, G. C. The two mucus layers of colon are organized by the MUC2 mucin, whereas the outer layer is a legislator of host–microbial interactions. *Proc. Natl. Acad. Sci. USA.* **108**, 4659–4665 (2011).

76. Vaishnava, S., Behrendt, C. L., Ismail, A. S., Eckmann, L. & Hooper, L. V. Paneth cells directly sense gut commensals and maintain homeostasis at the intestinal host-microbial interface. *Proc. Natl. Acad. Sci. USA.* **105**, 20858–20863 (2008).

77. Chae, S. A., Du, M., Son, J. S. & Zhu, M. J. Exercise improves homeostasis of the intestinal epithelium by activation of apelin receptor–AMP-activated protein kinase signalling. *J. Physiol.* **601**, 2371–2389 (2023).

Acknowledgements

Author contributions

H.J. and S.L. performed the single-cell RNA sequencing, figure preparation, and manuscript writing. Y.K., Y.K., and S.S. conducted the mouse experiments, including the power and endurance tests. Y.L. and M.K. prepared the ileum and conducted the preparation for single cell RNA sequencing. E.K., E.L., B.M.S., and H.C. analyzed the IHC results and assisted with manuscript writing. N.H. and J.K. were responsible for the experimental design. S.H. and B.H. participated in the analysis of single-cell RNA sequencing and provided significant input on the analytical methods. C.M.O. and S.F. supervised the research and wrote the manuscript.

Competing interests

The authors declare no competing interests.

Additional information

Supplementary information The online version contains supplementary material available at https://doi.org/10.1038/s41514-025-00242-z.

Correspondence and requests for materials should be addressed to Chang-Myung Oh or Sungsoon Fang.

Reprints and permissions information is available at http://www.nature.com/reprints

Publisher's note Springer Nature remains neutral with regard to jurisdictional claims in published maps and institutional affiliations.